ENCLOSED THERMAL MANAGEMENT METHOD FOR HIGH-POWER PHOTOVOLTAIC INVERTERS BASED ON HEAT PIPE HEAT SINK

by

Ziying ZHANG, Yupeng XIAN, Lu YANG, Xiangfen BIAN, Yannan LI, and Hanzhong TAO*

School of Energy Science and Engineering, Nanjing Tech University, Jiangsu, China

Original scientific paper
https://doi.org/10.2298/TSCI240512182Z

Photovoltaic inverter plays a crucial role in photovoltaic power generation. For high-power photovoltaic inverter, its heat loss accounts for about 2% of the total power. If the large amount of heat generated during the operation of the inverter is not dissipated in time, excessive temperature rise will reduce the safety of the devices. This paper proposes a closed photovoltaic inverter structure based on heat pipe and liquid cooling which overcomes the noise, dust and other problems caused by traditional air-cooling heat dissipation method and reduces cost of the volume occupied inside the body. Heat is dissipated through heat pipes, which are efficient heat transfer units. A simulation model of the actual cabinet was established using CFD, and the maximum junction temperature in the inverter was investigated under different coolant temperatures, flow rates, cooling liquid, and heat loads. The results showed that the liquid cooling heat dissipation structure can effectively dissipate the heat inside the cabinet. The impact of two different types of heat sink used for power modules on temperature uniformity was studied. The results indicated that the 9-heat pipe type heat sink has better heat dissipation and uniform hot spots performance, the maximum heat source temperatures in the chip and capacitor were reduced by 9.91 °C and 7.49 °C, respectively. Finally, the performance of the two types of radiators under different heat loads was studied.

Key words: *heat pipe heat sink, photovoltaic inverter, enclosed, thermal management, liquid cooling*

Introduction

The photovoltaic (PV) power plants are generally large-scale and not easily serviced frequently [1]. For PV systems, the stability and safety of the inverter are very important. Electronic components are very sensitive to temperature, and uneven temperature distribution and random hotspots are the main challenges in electronic thermal management [2]. As a power component, insulated gate bipolar transistor (IGBT) plays the role of power conversion and energy transmission in inverters. Since the invention of IGBT in 1980, it has been significantly optimized and improved in size and power [3]. However, along with these advancements comes the issue of temperature rise due to increased power density. Excessive temperatures

*Corresponding author, e-mail: taohanzhong@njtech.edu.cn

significantly diminish the service life of electronic components [4], making heat dissipation a hot point in electronic component research.

For electronic devices such as PV inverters, the most common heat dissipation method is air cooling. For some low-power inverters, natural convection demonstrates its advantages in terms of cost and space utilization [5-7]. However, with the rise of the inverter's power, natural convection cannot meet the heat dissipation needs, and the forced air cooling has a higher heat dissipation performance compared to natural convection, which is more widely used. Li *et al.* [8] and Biinnagel *et al.* [9] proposed adding deflectors to improve the cooling air-flow between the fins, aiming to solve the problem of low heat dissipation in fin radiators. Chu *et al.* [10] investigated a new type of plate fin heat sink. Experiments showed that the heat sink enhanced the heat transfer and reduced the thermal resistance by 5.5%-7.2% under a thermal load of 250 W. In addition, the triangular fins were better than the rectangular fins in terms of heat transfer. Lin *et al.* [11] proposed a new type of heat sink with rectangular and arc-shaped grooves for IGBT thermal management based on the traditional rectangular air-cooling fins. The results showed that the performance of the new type of heat sinks was better than that of the traditional fins.

However, in most cases, forced air-cooling requires a larger internal volume within the inverter to accommodate fans and heat sinks, and it also presents issues such as noise and dust. In contrast, liquid-cooling has been proven to have more advantages [12]. In addition to the improvement of the design of the liquid-cooled plate [13, 14], the researchers have made a lot of innovations in the cooling method. Xu *et al.* [15] developed a coupled model integrating heat conduction and coolant flow for high-power IGBT modules employing a double-sided liquid-cooling packaging structure. Results indicated that within a specified range, higher coolant flow rates led to improved cooling effect, albeit with increased flow resistance. Furthermore, the authors suggested that optimizing the material on the outlet surface of the flow channel could alleviate high chip temperatures at the outlet. Tiwarit *et al.* [16] proposed that installing a rotating impeller in a liquid-cooled plate can enhance heat transfer but will bring about a sharp increase in pressure drop in the flow channel. Future research is expected to improve this situation by modifying the blade shape. Wen *et al.* [17] proposed the use of nanofluids for immersion liquid-cooling of data center servers. Xue *et al.* [18] proposed a liquid jet cooling heat sink for heat dissipation of electronic chips and investigated the influence of different opening apertures on the thermal and hydraulic performance. As a result, the heat sink with small surface opening apertures have better thermal performance and uniform temperature, but increases the pressure loss of the heat sink, and for this purpose three parameter structures were applied to optimize the pressure loss. The fluid-flow chambers of these three structures have cross-sections that are slanted, convex, and concave, respectively.

Based on the previous literature, both air-cooling and liquid-cooling are widely used in electronic heat dissipation. Although these methods have shown excellent heat dissipation effects, they also present their own respective challenges. Considering the application scenarios of PV inverters, air-cooling method increases the additional load and is easy to accumulate dust, which is not conducive to the long-term operation of the device. The liquid cooling method may cause leakage due to its flow and corrosion, thus reducing the safety of the device. In addition, with the continuous updating of electronic devices, electronic components are becoming more sophisticated and compact, which requires more efficient cooling methods.

The application of heat pipes in electronic products has gradually attracted attention. Heat pipe is a closed heat transfer element with high heat transfer efficiency. The feasibility and effectiveness of using heat pipes for electronic heat dissipation have been proven by many

studies [19-21]. Researchers have made many innovations in the structure of heat pipes. Mizutani *et al*. [22] investigated and designed an ultrathin lamellar circulating heat pipe (LHP) for cooling mobile devices. They found that the maximum thermal performance of the LHP can reach 10 W/cm^2 during horizontal operation, and the minimum thermal resistance and effective thermal conductivity coefficients were 2.51 K/W and 2438 W/mK, respectively. Xia *et al*. [23] proposed and designed a closed thermal management solution based on a heat pipe heat sink, and designed two types of heat pipes (*U*-type and *L*-type). The results showed that the *L*-type was demonstrated superior effectiveness, leading to reductions in average temperatures of the low-power chip and high-power chip by 10 °C and 5.9 °C, respectively. Ren *et al*. [24] developed a *U*-shaped micro heat pipe array for battery thermal management, which improves the temperature uniformity of the battery module during operation. Additionally, many studies have developed various cooling systems or heat sinks based on heat pipes. Behi *et al*. [25] introduced a horizontal PCM-assisted heat pipe system for electronic heat dissipation. They studied the liquid phase fraction and temperature distribution of the PCM during the working process under different heating powers. The results showed that in the power range of 50-80 W, this system can achieve 86.7% heat dissipation effect. Han *et al*. [26] proposed a novel cooling device with a loop heat pipe composite heat sink. The study found that the hot spot temperature was reduced and the temperature uniformity of the electronic components was optimized with the addition of graphene copper foil. Zachariae *et al*. [27] investigated an air-cooled heat sink for traction inverters, demonstrating that the heat sink is suitable for medium-sized passenger vehicles with thermal loads exceeding 2.2 kW. Li *et al*. [28] applied metal foam in heat pipe heat sinks to enhance the heat transfer between the heat pipe condenser section and the air. Experiments showed that the metal foam heat pipe heat sink outperforms traditional finned heat pipe heat sinks by a factor of four in overall performance, making it more suitable for compact cooling systems.

Based on the research review, both air-cooling and liquid-cooling are inevitably defective. Most of the current researches have adopted a single heat dissipation method and focused on the heat dissipation inside the cabinets, which does not adequately address concerns related to dustproofing and safety of inverters. This paper proposes a liquid-cooling structure based on heat pipe heat sink and designs a closed thermal management scheme under this structure to effectively address these problems. The method of CFD was utilized to investigate the thermal performance of this design.

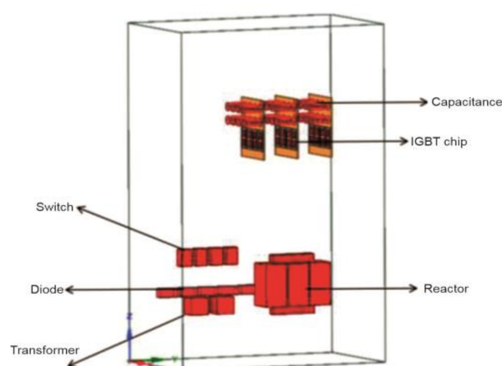

Figure 1. Simplified model of PV inverter

Methodology

Physical model

In this paper, a 500 kW high-power PV inverter is taken as the research object, the simulation model of PV inverter is shown in fig. 1, with a cabinet size of 1200 mm × 700 mm × 2000 mm. The inverter contains power components such as inverter module, capacitor, reactor, transformer and so on. The specific heat loss of each component is shown in tab. 1. Among them, each inverter module in the inverter includes four IGBT modules with each IGBT module containing two IGBT chips, each with a power loss of 335W.

Table 1. The heat loss of the main component in the inverter

Device name	Power [W]	Number	Total power [W]
Inverter modules (8 IGBT chips and 8 capacitance each)	335 × 8 = 2680 8 × 16 = 128	3	2808 × 3 = 8424
Anti-reflection diode	205	5	1025
Transformers	100	2	200
Reactor	1500	1	1500
Switch	60	4	240
			11389

In this paper, only the temperature field inside the inverter is studied, so only the cabinet and main heating components are modeled. To reduce the computational resources, regular rectangles, cylinders and other shapes are used instead of the actual elements as the body heat source for uniform heat generation when the thermal analysis is carried out for the whole inverter. Considering that the inverter module is the component with the highest heat generation within the system, efforts are made to align the geometric modeling with realistic outcomes. As part of the geometric modeling process, this paper accounts for the thermal resistance of different material layers within the IGBT module, establishing an IGBT thermal resistance model. The specific dimensions and materials are presented in tab. 2.

Table 2. The IGBT module parameters

Layer	Material	Thickness [mm]	Density [kgm^{-3}]	Thermal conductivity [Wm^{-1}K^{-1}]
IGBT chip	Si	0.15	2329	139
IGBT chip solder	Sn-Ag-Cu	0.1	7400	78
DCB copper	Cu	0.38	8960	387.6
DCB ceramic	Al_2O_3	0.3	3690	30
DCB copper	Cu	0.25	8960	387.6
Baseplate solder	Sn-Ag-Cu	0.15	7400	78
Baseplate	Cu	3	8960	387.6

Table 3. Size of heat sink

Name	Material	Size
Heat sink substrate	Aluminum	δ = 20 mm Cross-sectional area adjusted to the size of the heat source
Heat pipe at inverter module	Copper	Outer diameter 10 mm, evaporation section 340 mm, condensation section 300 mm, and total length 1350-1550 mm
Heat pipes at reactors, switches, and transformers	Copper	Evaporation section 500 mm, condensation section 300 mm, and total length 1400 mm
Heat pipe at diode	Copper	Evaporation section 150 mm, condensation section 150 mm, and total length 650 mm

This research aims to design a heat dissipation structure for a fully enclosed PV inverter cabinet. The main idea is to dissipate heat to the outside of the cabinet through heat pipes. According to the different power of the internal components, a heat pipe heat sink with the suitable number of heat pipes is installed on the back of these components. The heat pipe heat sink consists of a 20 mm substrate with some 10 mm diameter heat pipes embedded inside, tab. 3. The condensation section of the heat pipe is uniformly led out from the back plate of the cabinet, and the cooling liquid is circulated externally to dissipate heat through the condensation

section of the heat pipe. For the place where power components are concentrated, we can use a single heat pipe heat sink to cooling all of them. The specific geometric model is shown in fig. 2. According to the distribution position of internal components and the arrangement position of heat pipes, this study sets up a total of three cooling liquid channels.

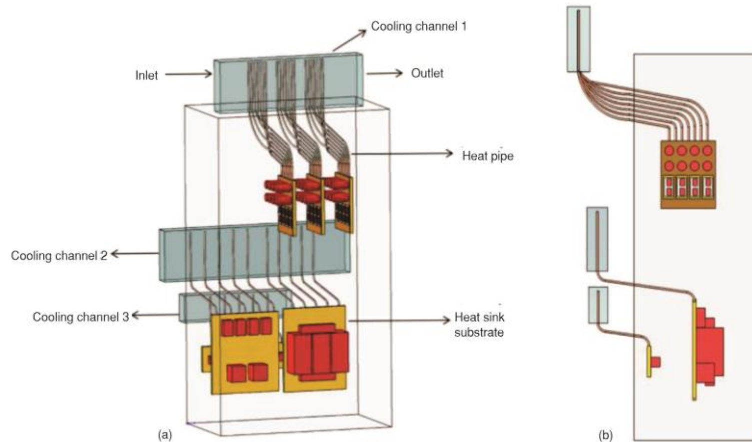

Figure 2. Thermal management scheme of PV inverter; (a) front view and (b) side view

Thermal resistance analysis of heat dissipation system

The main heat source of the IGBT module is the IGBT chip, and its detailed structure is shown in fig. 3. The module mainly includes three types of thermal resistance, R_{jc} the thermal resistance from the chip to the case, R_{hs} the thermal resistance from the case to the heat sink, and R_{ha} the thermal resistance from the heat sink to the environment. Based on the thermal resistance model, this paper established actual models of the chip, DCB board and copper substrate for the IGBT module, and considered the influence of solder thermal resistance through the shell thermal conduction model. Figure 4 illustrates the thermal resistance network model of a single heat sink at the power module in this model. Taking one of the IGBT chips as an example, the thermal resistance between chip and the cooling medium can be divided into five

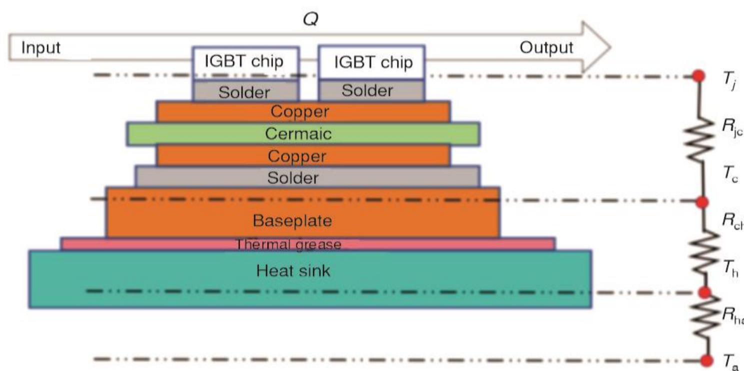

Figure 3. The IGBT thermal resistance model

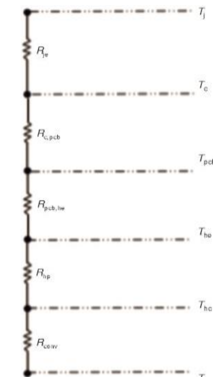

Figure 4. Thermal resistance networks for heat sinks

parts, R_{jc} the thermal resistance from chip to case, $R_{c,PCB}$ the thermal resistance from the case to PCB, $R_{PCB,he}$ the thermal resistance from PCB to the evaporation section of the heat pipe, R_{hp} the thermal resistance of the heat pipe, and R_{conv} the convection thermal resistance between the heat pipe condensation section and the coolant.

Numerical methods

Governing equations

Based on the following assumptions, a computational model of the liquid-cooled heat sink was established:

- The final result of the model is in steady state.
- Air is treated as an incompressible fluid, with its properties remaining constant except for density fluctuations.
- The heat generating element inside the cabinet is assumed to be a body heat source that generates heat uniformly.
- Thermal radiation inside the cabinet is not considered.

Considering the previous assumptions, based on the conservation of mass, momentum, and energy, the following governing equations of flow were solved:

Mass conservation equation

$$\nabla\left(\rho u\right)=0 \tag{1}$$

Momentum conservation equation

$$\nabla\left(\rho u^{2}\right)=-\nabla p+\mu\nabla^{2}u-\nabla\left(\rho\overline{u'u'}\right) \tag{2}$$

Energy conservation equation

$$\rho c_{p}\left(u\nabla T\right)=k\nabla^{2}T+\nabla\left(\frac{u_{t}}{\mathrm{Pr}_{t}}\nabla T\right) \tag{3}$$

where ρ is the fluid density, p – the pressure, μ – the hydrodynamic viscosity, u – the velocity, $\overline{u'u'}$ – the Reynolds stress tensor, which accounts for the additional stresses due to turbulence, k – the thermal conductivity of the fluid, c_p – the specific heat capacity, T – the temperature, u_t – the turbulent viscosity, and Pr_t – the turbulent Prandtl number.

The Reynolds numbers need to be calculated before the simulation calculation. The Reynolds number in cooling channel is calculated as:

$$\mathrm{Re}=\frac{\rho_{c}vd}{\mu_{c}} \tag{4}$$

where ρ_c is the density of cooling liquid, v – the velocity, d – the heat pipe diameter, and μ_c – the cooling liquid viscosity. When the inlet velocity of cooling liquid is set in increments of 1 m/s from 2-10 m/s, the value of the Reynolds numbers is between 19904-99521. Therefore, the fluid model used is the turbulence model.

Simulation methods and boundary conditions

The numerical simulation is carried out in ANSYS FLUENT, and the simulation was performed on a computer with 48 cores and 192 GB of memory. The solution method used the Coupled algorithm, which is more suitable for steady-state calculations because it has the advantage of being robust for calculating single phase flows. The momentum and energy

equations adopt the second-order windward discretization format, and the turbulence model adopts the standard k-epsilon model, which is the most widely used in engineering; it is stable and relatively accurate. So this model is used for numerical simulations under turbulent flow conditions.

The inlet of the cooling channel was set as a velocity inlet, and the outlet was set as a pressure boundary condition. The relaxation factors for pressure, momentum, and energy were set to 0.5, 0.5, and 0.75, respectively. The residual for energy was set to 10^{-6}, while the residuals for all other variables were set to 10^{-3}. After approximately 500 iterations, all reached the convergence criteria.

Model validation

To verify the reliability of this numerical simulation model and results, this paper conducts model verification on the simulation done by Lu *et al.* [29], using the same geometric model and initial conditions as in the literature for the heat pipe radiator used in the IGBT module. For verification analysis, we selected the effect of cooling fluid temperatures on the maximum temperature of IGBT in the article as the verification object. As shown in fig. 5, the results indicate that the disparity between the simulation results and the original data does not exceed 10%, which demonstrates the reliability of the numerical simulation method used in this paper on the existing model. This paper will use the same numerical simulation method as the reference for subsequent simulation calculations.

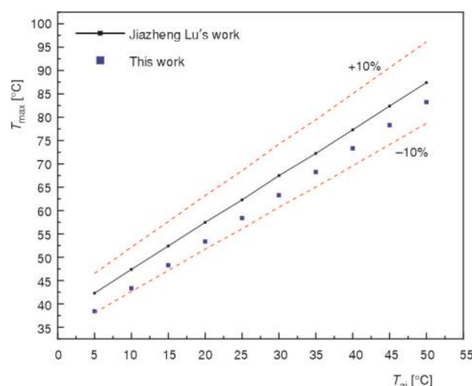

Figure 5. Model validation

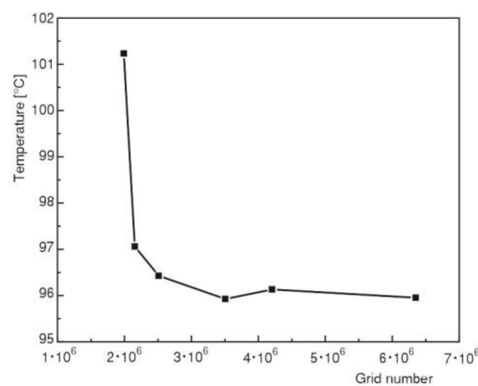

Figure 6. Grid independence test

Grid independence test

Grid independence verification is to ensure that the calculation results of our model do not significantly change due to the size or density of the grid. Since conducting grid independence research on the entire cabinet requires a large amount of computing resources, we selected an inverter module in the cabinet to conduct grid independence research. As shown in fig. 6, we compared the results under six different mesh counts, using the maximum junction temperature of the IGBT as the study subject. The specific results are shown in tab. 4. When the mesh count increased from 3.5 million to 4.2 million, the results varied by only 0.22%, which is within an acceptable range. Further increasing the mesh count had an insignificant effect on the calculation results. Therefore, we used the mesh division method with 3.5 million meshes for a single module to perform the mesh division for the overall model, ultimately determining the total mesh count to be 12.1 million.

Table 4. Grid independence test results

Grid number [$\times 10^4$]	Junction temperature of IGBT [°C]	Deviation [%]
198.9	101.23	–
215.5	97.06	4.12
250.9	96.43	0.65
350.6	95.93	0.52
420.5	96.13	0.22
635.1	95.95	0.19

Results and discussions

To preliminary study the feasibility of the proposed heat dissipation design, we conducted simulations under the conditions of an inlet water temperature of 20 °C, and a flow rate of 5 m/s. Traditional forced air-cooling methods may result in non-uniform flow fields, leading to uneven heat dissipation [11, 23]. The heat dissipation method used in this article can independently cool heat sources at different locations, and each heat dissipation zone does not affect each other. Figure 7(a) shows the temperature contour of each power component in the inverter cabinet when T_{ai} = 25 °C. It can be seen that the temperatures of reactors, switches, transformers and diodes are well controlled, and their maximum temperatures are 39.74 °C, 26.41 °C, 27.81 °C, and 48.7 °C, respectively. Their maximum temperatures are far less than their respective maximum temperature resistance values, which meets the requirements of thermal management. The inverter module in the cabinet has the highest temperature, and the maximum temperature of IGBT is 85.88 °C. According to the working requirements of the IGBT chip, the maximum junction temperature must not be higher than 150 °C [3]. The maximum temperature

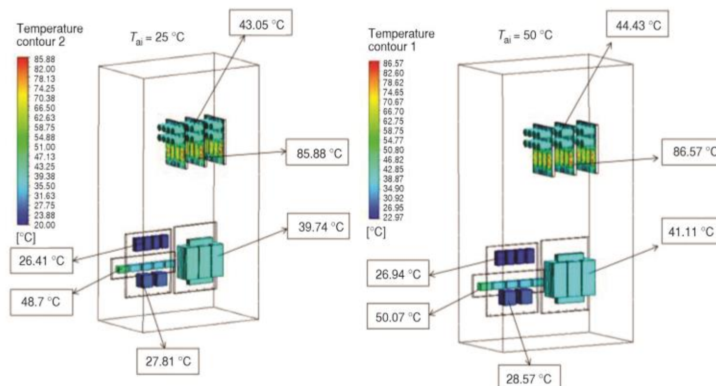

Figure 7. Temperature contour inside the inverter under two different ambient temperatures; (a) T_{ai} = 25 °C and (b) T_{ai} = 50 °C

of the capacitor is 43.05 °C, which is less than its maximum temperature resistance value of 85 °C [30]. This heat dissipation design meets the requirements under this heat load, which proves the feasibility of the heat pipe liquid-cooling solution. In order to study the impact of environment temperature, we also simulated the heat dissipation effect of this design under extreme environmental conditions (50 °C), the results are shown fig. 7(b). The maximum temperature of each component in this environment compared to the ambient temperature of 25 °C is not much difference, only 0.5-2 °C or so, which is due to the heat generation of chip is directly dissipated by the cooling medium through the heat pipe heat sink. In contrast, the amount of

heat dissipated by thermal convection when the heat source contacts with air is relatively small, which indicates that this cooling method can be applicable in many extreme weather conditions.

According to the previous research, we found that the inverter module in the cabinet is the component with the highest power and temperature rise. Therefore, in the subsequent research in this paper, we refrain from extensive discussion on other heat sources and instead focus on the temperature rise and heat dissipation at the inverter module location. In thermal design, the maximum junction temperature of the IGBT module typically serves as the primary criterion. Relevant literature indicates that in the inverter, the IGBT modules and capacitors are the most vulnerable components [30, 31]. This article considers the maximum junction temperature of the inverter module as a key metric for assessing heat dissipation effectiveness.

Effect of inlet coolant temperature on heat dissipation performance

In this study, water was employed as the coolant to investigate the temperature rise of the inverter module under various inlet conditions. Specifically, simulations were conducted with inlet flow velocities set at 5 m/s, while the inlet water temperatures varied from 10 °C to 35 °C in increments of 5 °C. Figure 8 illustrates the temperature contour of a representative inverter module at different inlet temperatures. We can conclude that the temperature rise of the inverter module is greatly affected by the cooling water temperature. Lower inlet cooling water temperatures correspond to better heat dissipation performance. As shown in fig. 9, it is observed that as the inlet temperature of the cooling water increases from 10 °C to 35 °C, the maximum junction temperature of the IGBT module shows an approximately linear increase, and the capacitor and heat sink base exhibit the same trend. The maximum junction temperatures of all components exhibit a linear increase with the rise in coolant inlet temperature. Furthermore, the impact of coolant inlet temperature on the

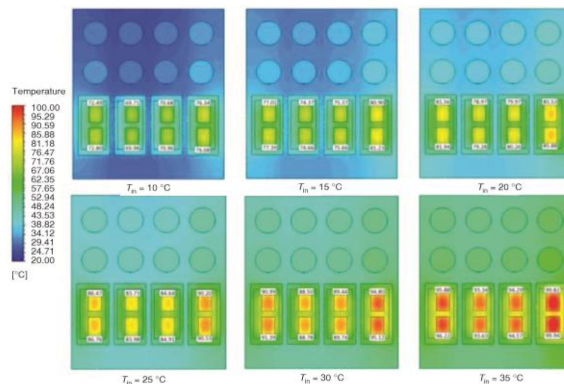

Figure 8. Temperature contour of the inverter module at different coolant temperatures

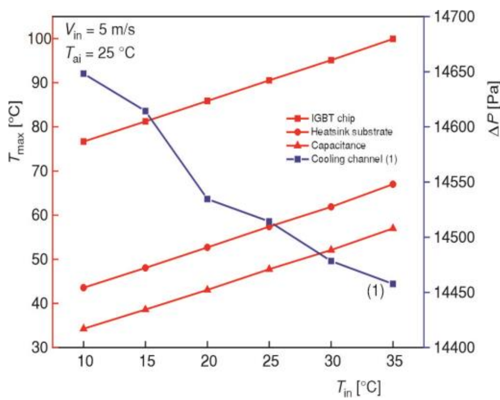

Figure 9. Effect of coolant inlet temperature on heat sink performance

pressure drop in the cooling channel is found to be relatively minor. Specifically, as the inlet temperature rises from 10 °C to 35 °C, the pressure drop decreases by only 190.59 Pa. This reduction in pressure drop is attributed to changes in the physical properties of the coolant due to temperature variation, notably the decrease in coolant viscosity with increasing temperature.

Effect of coolant flow rate on heat dissipation performance

In the scenario where the cooling water temperature is held constant at 20 °C, we conducted an investigation into the impact of coolant flow velocity on heat sink performance. As shown in fig. 10(a), the maximum junction temperature of the IGBT module decreases as the cooling water velocity increases, although the relationship of this change is not linear. Significantly, increasing the coolant flow velocity from 2-6 m/s significantly enhances heat dissipation. However, further escalation of coolant flow velocity results in diminishing returns in heat dissipation enhancement. Figure 10(b) provides insights into this phenomenon, as Reynolds number increases, there is a corresponding rise in the Nusselt number, indicating that the increase in flow rate improves the heat transfer and reduces the convective thermal resistance between the cooling fluid and the heat pipe. However, once Reynolds number surpasses a certain threshold, the incremental increase in Nusselt number gradually diminishes, which implies that the enhanced heat transfer effect resulting from increased flow velocity attenuates as the velocity continues to rise. In fig. 10(a), it is evident that higher flow velocities correspond to increased pressure drops of the coolant. Pressure drop serves as a crucial technical-economic indicator of energy loss within the system [32]. A greater pressure drop implies a higher energy requirement for the system. Therefore, a coolant flow velocity within the range of 4-6 m/s emerges as a preferable option.

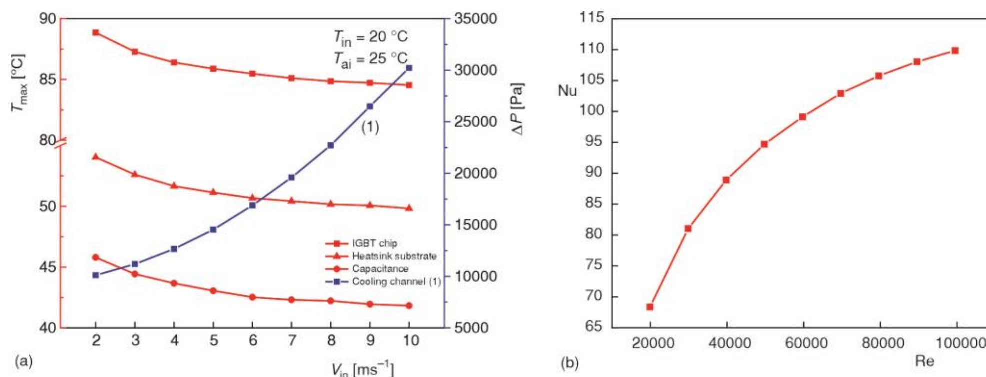

Figure 10. Effect of coolant flow rate on heat sink performance; (a) effect on component temperature and channel pressure drop and (b) relationship between Reynolds and Nusselt numbers

Effects of different cooling liquid on heat dissipation performance

During the winter in northern regions, the ambient temperature may drop below 0 °C, using water as a coolant medium under such conditions poses the risk of pipeline freezing, for this reason, our study examines the influence of alternative coolant mediums on heat dissipation performance. Ethylene glycol-water solution is a common antifreeze coolant. We conducted simulations to investigate operating conditions using 50% ethylene glycol-water solution and 50% ethylene glycol-water nanofluid with 0.05 volume fraction of Al_2O_3 [33] as coolant

mediums. The results, depicted in fig. 11, reveal that water exhibits superior cooling performance compared to the other two coolant mediums, in the absence of environmental factors, water remains the optimal choice due to its higher specific heat capacity and thermal conductivity relative to the other fluids. However, considering the limitations imposed by ambient temperatures, the use of antifreeze coolant may partially compromise heat dissipation effectiveness, this result is consistent with previous research [34]. Adding nanofluids to the ethylene glycol-water solution can enhance heat dissipation, but the effect of enhanced heat transfer is not significant. For a 50% ethylene glycol-water solution, the heat dissipation improvement is less than 2%, while it significantly increases the cost without proportional benefits, thus lacking cost-effectiveness. Therefore, ethylene glycol solution emerges as a comparatively suitable antifreeze coolant. Accordingly, we emphasize the comparative analysis of different concentrations of ethylene glycol solutions on heat dissipation effectiveness.

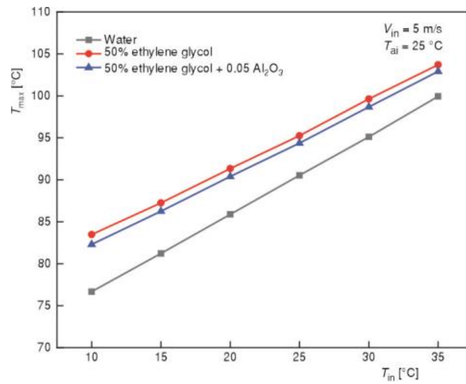

Figure 11. Maximum IGBT temperature with different inlet temperature under different cooling liquid

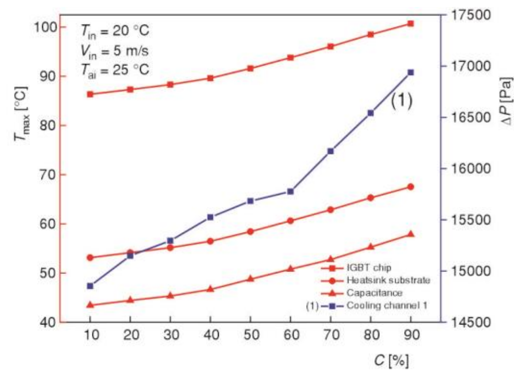

Figure 12. Effect of ethylene glycol concentration on heat sink performance

We investigated the effect of varying concentrations of ethylene glycol on the performance of the heat sink under a coolant velocity of 5 m/s and an inlet temperature of 20 °C. As shown in fig. 12, an increase in the concentration of ethylene glycol in the coolant leads to a gradual and increasingly significant rise in the maximum temperatures of the components. This trend is attributed to the reduction in the specific heat capacity and thermal conductivity of the coolant with higher concentrations of ethylene glycol, consequently diminishing the heat transfer effect of the coolant. Moreover, the viscosity of the coolant increases proportionally with the elevation of ethylene glycol concentration, which leads to a gradual increase in the cooling pressure drop. Hence, the elevation in ethylene glycol concentration does not favor the improvement of heat dissipation performance. Table 5 provides the physical properties of ethylene glycol coolant at 20 °C for various concentrations. Generally, winter temperatures do not plummet below –35 °C, suggesting that a 50% concentration of ethylene glycol solution is relatively suitable.

Optimized design for temperature uniformity

In addition to evaluating heat dissipation capability based on the maximum junction temperature, temperature uniformity has emerged as a crucial parameter to consider. In the realm of electronic chips, excessive temperature gradients and localized hotspots can precipitate problems such as thermal strain and performance degradation [2]. We observed variations in

Table 5. Physical properties of ethylene glycol at various concentrations

C [%]	ρ [kgm^{-3}]	C_p [Jkg^{-1}K^{-1}]	λ [Wm^{-1}K^{-1}]	μ [kgm^{-1}s^{-1}]	Freezing point [°C]
10	1013.34	3972	0.545	1.21×10^{-3}	–3.2
20	1029.72	3815	0.497	1.65×10^{-3}	–7.8
30	1045.25	3645	0.453	2.2×10^{-3}	–14.1
40	1059.68	3468	0.415	2.96×10^{-3}	–22.3
50	1073.35	3281	0.38	3.94×10^{-3}	–33.8
60	1086.27	3084	0.349	5.38×10^{-3}	–48.3
70	1098.48	2878	0.322	7.53×10^{-3}	–
80	1110.13	2663	0.298	1.005×10^{-2}	–46.8
90	1121.23	2438	0.276	1.295×10^{-2}	–29.8

the maximum temperature of each IGBT chip in this study, which is related to the spacing and the number of heat pipes in the substrate. Since the IGBT chips are mounted equidistantly on the module and the size of the heatsink substrate needs to be the same as the size of the PCB board, the installation positions of the heat pipes in the substrate are uniformly spaced to ensure homogeneous heat dissipation. In the initial model, the heat sink substrate at the inverter module is lined up with seven heat pipes. To evaluate how altering the number of heat pipes affects the temperature consistency of the inverter module, we conducted a comparative analysis of the maximum temperatures observed for each IGBT chip and capacitor. This comparison was conducted under two conditions: with seven and nine heat pipes arranged on the substrate. For clarity and ease of reference, each component on the module was systematically numbered, as illustrated in fig. 13(b).

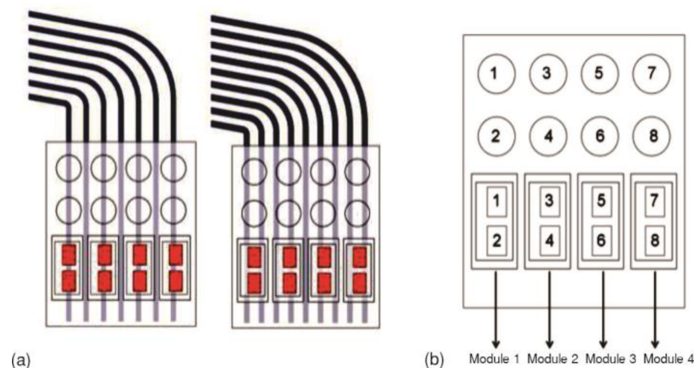

Figure 13. (a) two heat sink configurations: 7 heat pipes type and 9 heat pipes type and (b) numbering of the components in the inverter module

As can be seen in figs. 14 and 15, the implementation of nine heat pipes type heat sink has significantly enhanced both the heat dissipation effectiveness and temperature uniformity of the inverter module. In comparison, under the seven heat pipes configuration, the temperature differences between IGBT chips and capacitors were 7.25 °C and 5.45 °C, respectively. Through optimization, these temperature differences were reduced to 2.89 °C and 2.84 °C, respectively, under the nine heat pipes configuration. Improving the cooling performance and temperature uniformity of the heat sink by increasing the number of heat pipes is effective, albeit accompanied by an increase in heat sink weight and cost, posing challenges for future consideration.

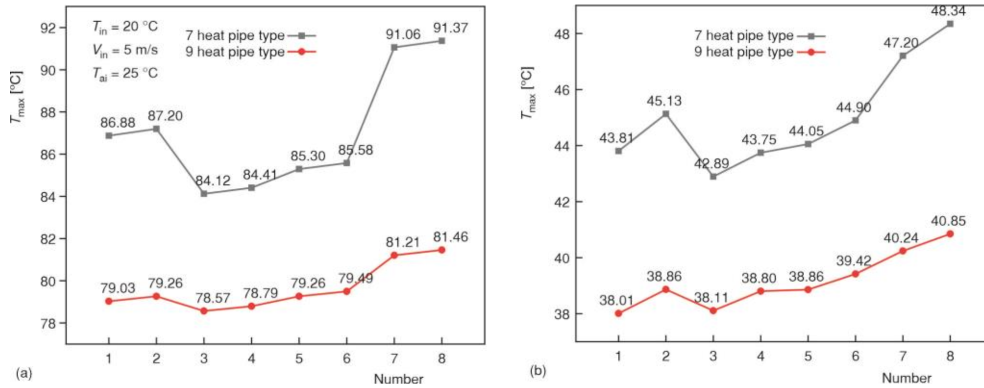

Figure 14. Optimization results for temperature uniformity; (a) IGBT chip temperature and (b) capacitor temperature

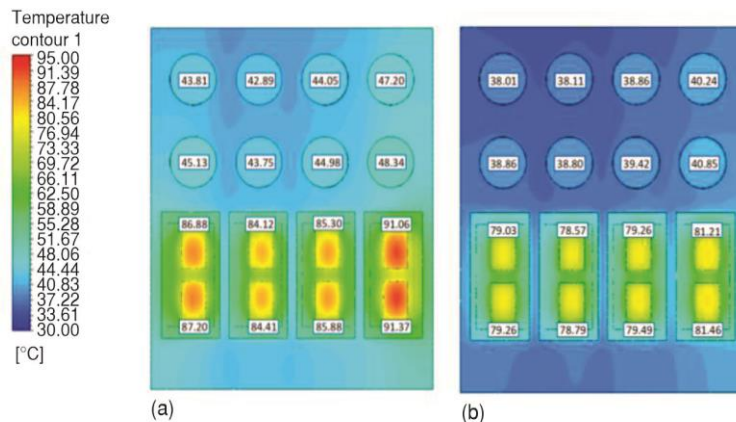

Figure 15. Temperature contour of inverter module for two heat sink configurations; (a) 7 heat pipes and (b) 9 heat pipes

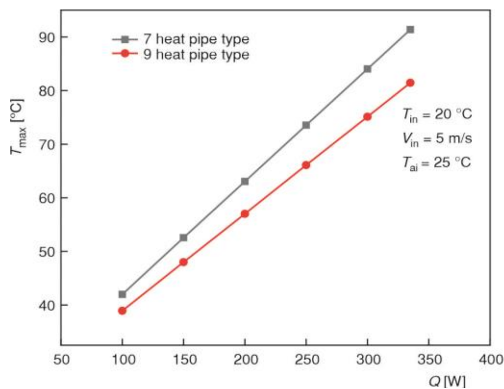

Figure 16. The maximum temperature of IGBT chips under different heat loads

Effect of heat load on heat dissipation performance

The heat power of a single IGBT chip in this model is 335 W, but under the actual operation of the PV inverter, the thermal load on the inverter module is dynamic rather than constant, the heat loss is positively correlated with solar irradiance [35]. Thus, this section conducts simulations to assess the maximum junction temperature of the IGBT modules within the inverter cabinet under varying thermal loads of 100 W, 150 W, 200 W, 250 W, 300 W, and 335 W, considering two distinct heat sink configurations. As shown in fig. 16, the maximum temperature of the inverter module demonstrates a linear relationship with power, exhibiting an increase of approximately 20 °C for every 100 W increment in power. The heat dissipation efficacy of the nine heat pipes configuration, in comparison to

the seven heat pipes configuration, becomes progressively more pronounced with escalating power levels. Specifically, at a thermal load of 100 W, the maximum temperature is reduced by 3.07 °C with nine heat pipes compared to seven heat pipes. Accordingly, at a thermal load of 335 W, the maximum temperature is reduced by 9.9 °C with nine heat pipes compared to seven heat pipes.

Conclusions

This paper introduces a thermal management solution for high-power PV inverter cabinets based on heat pipes, aiming to achieve enclosed, efficient, and safe heat dissipation. The feasibility of this cooling approach is substantiated through measurements of the maximum junction temperature within the cabinet. Key research outcomes are delineated as follows.

- The PV inverters require protection against environmental dust and debris ingress. The proposed cooling solution utilizes heat pipes as thermal conduits between the internal component and the external cooling liquid, facilitating effective heat dissipation while preserving the enclosure integrity of the internal cabinet. Moreover, the independent operation of heat dissipation units within the system enhances equipment reliability. This approach demonstrates pronounced cooling performance for devices with lower heat dissipation requirements.
- The heat dissipation effectiveness of a cooling system is influenced by cooling flow rate, coolant temperature and coolant medium. Increasing the cooling flow rate improves heat dissipation effect but concurrently increases pressure drop. Optimal cooling flow rates fall within the range of 4-6 m/s. Lower coolant temperatures correspond to reduced maximum temperatures within the cabinet. Furthermore, different coolant mediums impact the heat dissipation performance of heat sink, with water exhibiting superior performance among the three considered mediums. In consideration of environmental factors, a 50% ethylene glycol solution is identified as the most suitable choice.
- Regarding the heat sink at the inverter module, the configuration employing nine heat pipes exhibits superior performance compared to the seven heat pipes structure. This configuration optimizes both the uniformity and performance of heat dissipation from the heat sink. Specifically, the maximum temperatures of the IGBT chips and capacitors are reduced from 91.37°C to 81.46°C and from 48.34°C to 40.85°C, respectively. Additionally, as the heat load steadily increases, the heat dissipation performance of the nine heat pipe structure becomes more pronounced.

Nomenclature

p – pressure [Pa]
Re – Reynolds number [–]
T – temperature [°C]
V – velocity [ms^{-1}]
Nu – Nusselt number [–]

Subscripts

ai – ambient
c – case
j – junction
f – cooling fluid
hc – condensation section of heat pipe
he – evaporation section of heat pipe
hs – heat sink

Acronyms

IGBT – insulate gate bipolar transistor
PCB – printed circuit board

References

[1] Falck, J., Felgemacher, C., *et al*., Reliability of Power Electronic Systems: An Industry Perspective, *IEEE Industrial Electronics Magazine*., *12* (2018), 2, pp. 24-35

[2] He, Z., *et al*., Thermal Management and Temperature Uniformity Enhancement of Electronic Devices by Micro Heat Sinks: A Review, *Energy*., *216* (2021), 119223
[3] Iwamuro, N., Laska, T., IGBT History, State-of-the-Art, and Future Prospects, *IEEE Transactions on Electron Devices*., *64* (2017), 3, pp. 741-752
[4] Andresen, M., *et al*., Review of Active Thermal and Lifetime Control Techniques for Power Electronic Modules, *Proceedings*, 16th European Conference on Power Electronics and Applications., Lappeenranta, Finland, 2014, Vol. 1, pp. 1-10
[5] Christen, D., *et al*., Energy Efficient Heat Sink Design: Natural Versus Forced Convection Cooling, *IEEE Transactions on Power Electronics*., *32*(2017), 11, pp. 8693-8704
[6] Rabkowski, J., *et al*., Design Steps Toward a 40-kVA SiC JFET Inverter with Natural-Convection Cooling and an Efficiency Exceeding 99.5%, *IEEE Transactions on Industry App*., *49* (2013), 4, pp. 1589-1598
[7] Bouknadel, A., *et al*., Comparative Study of Fin Geometries for Heat Sinks in Natural Convection, *Proceedings*, 2014 International Renewable and Sustainable Energy Conference (IRSEC)., Ouarzazate, Morocco, 2014, Vol. 1, pp. 723-728
[8] Li, G., *et al*., Thermal Analysis and Structural Optimization of Dual IGBT Module Heat Sink under Forced Air Cooling Condition, *Proceedings*, 3rd Advanced Information Management, Communicates, Electronic and Automation Control Conference (IMCEC)., Chongqing, China, 2019, Vol. 1, pp. 1757-1762
[9] Bunnagel, C., *et al*., Forced Air Cooled Heat Sink with Uniformly Distributed Temperature of Power Electronic Modules, *Applied Thermal Engineering*., *199* (2021), 117560
[10] Chu, W, X., *et al*., CFD Analysis and Experimental Verification on a New Type of Aircooled Heat Sink for Reducing Maximum Junction Temperature, *Int. J. Heat Mass Transf*., *148* (2019), 119094
[11] Lin, X., *et al*., Design and Analysis of the IGBT Heat Dissipation Structure Based on Computational Continuum Mechanics, *Entropy*., *22* (2020), 8, pp. 816-828
[12] Joshua, E., *et al*., Liquid-Cooled Heat Sink Design for a Multilevel Inverter Switch with Considerations for Heat Spreading and Manufacturability, *Applied Thermal Engineering*., *219* (2023), 119588
[13] Kadir, G., *et al*., A Novel Cooler Block Design for Photovoltaic Thermal Systems and Performance Evaluation Using Factorial Design, *Journal of Building Engineering*., *48* (2021), 103928
[14] Wei, H., *et al*., Performance Analysis and Structural Optimization of a Finned Liquid-Cooling Radiator for Chip Heat Dissipation, *Applied Energy*., *327* (2022), 120048
[15] Xu, Y., *et al*., Heat Dissipation Simulation of Double-sided Liquid-cooled IGBT Module Package, *Proceedings*, 20th International Conference on Electronic Packaging Technology(ICEPT)., Hong Kong, China, 2019, Vol. 1, pp. 1-4
[16] Tiwari, R., *et al*., Enhancement of Heat Transfer in Liquid-Cooled Heat Sink Using Rotating Impeller, in: *Lecture Notes in Mechanical Engineering*., Beach Road, Singapore, 2022
[17] Wen, S., *et al*., Simulation Study on Nanofluid Heat Transfer in Immersion Liquid-Cooled Server, *Applied Sciences*., *13* (2023), 13, 7575
[18] Xue, Z, G., *et al*., Thermal-Hydraulic Performance Analysis of a Liquid-Jet-Cooled Heat Sink with a Macroscopic Porous Flow Diverter, *Applied Thermal Engineering*., *230* (2023), 120654
[19] Marshall, G, J., *et al*., Thermal Management of Vehicle Cabins, External Surfaces, and Onboard Electronics: An Overview, *Engineering*., *5* (2019), 5, pp. 954-969
[20] Mochizuki, M., Latest Development and Application of Heat Pipes for Electronics and Automotive, *Proceedings*, IEEE CPMT Symposium Japan (ICSJ)., Kyoto, Japan, 2017, Vol. 1, pp. 87-90
[21] Laloya, E., *et al*., Heat Management in Power Converters: From State of the Art to Future Ultrahigh Efficiency Systems, *IEEE Transactions on Power Electronics*., *31* (2016), 11, pp. 7896-7907
[22] Mizutani, T., *et al*., Experimental and Analytical Investigation of a 0.3-mm-Thick Loop Heat Pipe for 10 W-Class Heat Dissipation, *International Journal of Heat and Mass Transfer*., *193* (2022), 122950
[23] Xia, G., *et al*., Thermal Management Solution for Enclosed Controller Used in Inverter Air Conditioner Based on Heat Pipe Heat Sink, *International Journal of Refrigeration*., *99* (2019), Mar., pp. 69-79
[24] Ren, R, Y., *et al*., Active Air Cooling Thermal Management System Based on U-Shaped Micro Heat Pipe Array for Lithium-Ion Battery, *Journal of Power Sources*., *507* (2021), 230314
[25] Behi, H., *et al*., Investigation of PCM-Assisted Heat Pipe for Electronic Cooling, *Applied Thermal Engineering*., *127* (2017), Dec., pp. 1132-1142
[26] Han, C, L., *et al*., Study of Heat Dissipation Characteristics of Loop Heat Pipe with Heat Sink Of Composite Material, *Applied Thermal Engineering*., *200* (2021), 117572
[27] Zachariae, J., *et al*., Silicon Carbide Based Traction Inverter Cooling in Electric Vehicle Using Heat Pipes, *Thermal Science and Engineering Progress*., *46* (2023), 102155

[28] Li, M ,S., *et al*., Experimental Study on Thermal and Flow Characteristics of Metal foam Heat Pipe Radiator, *International Journal of Thermal Sciences*., *159* (2021), 106572
[29] Lu, J., *et al*., Investigation of a Rectangular Heat Pipe Radiator with Parallel Heat Flow Structure for Cooling High-Power IGBT Modules, *International J. of Thermal Sciences*., *135* (2019), Jan., pp. 83-93
[30] Wang, H., *et al*., Transitioning to Physics-of-Failure as a Reliability Driver in Power Electronics, *IEEE Journal of Emerging and Selected Topics in Power Electronics*., *2* (2014), 1, pp. 97-114
[31] Lima, G, P, De., *et al*., Thermal Mathematical Modeling of Photovoltaic Inverters and Experimental Validation, *Proceedings*, Brazilian Power Electronics Conference (COBEP)., Joao Pessoa, Brazil, 2021, Vol. 1, pp. 1-7
[32] Zhang, Z., *et al*., Optimal Design of Multi-channel Water Cooled Radiator for Motor Controller of New Energy Vehicle, *CES Transactions on Electrical Machines and Systems*., *6* (2022), 1, pp. 87-94
[33] Heris, S, Z., *et al*., Experimental Investigation of Convective Heat Transfer of Al_2O_3/Water Nanofluid in Circular Tube, *International Journal of Heat and Fluid Flow*., *28* (2007), 2, pp. 203-210
[34] Habibian, S, H., *et al*., Numerical Investigation of the Effects of Fin Shape, Antifreeze and Nanoparticles on the Performance of Compact Finned-Tube Heat Exchangers for Automobile Radiator, *Applied Thermal Engineering., 133* (2018), Mar., pp. 248-260
[35] He, J, K., *et al*., Thermal Performance Evaluation of 1500-VDC Photovoltaic Inverters Under Constant Power Generation Operation, *Proceedings*, IEEE Conference on Power Electronics and Renewable Energy (CPERE)., Aswan, Egypt, 2019, Vol. 1, pp. 579-583

Paper submitted: May 12, 2024
Paper revised: June 20, 2024
Paper accepted: JUne 28, 2024

.
2025 Published by the Vinča Institute of Nuclear Sciences, Belgrade, Serbia.
This is an open access article distributed under the CC BY-NC-ND 4.0 terms and conditions.